Independent Blade Pitch Controller Design for a Three-Bladed Turbine Using Disturbance Accommodating Control

Preprint

Na Wang, Alan D. Wright, and
Kathryn E. Johnson
National Renewable Energy Laboratory

Presented at the 2016 American Control Conference
Boston, Massachusetts
July 6–8, 2016

NREL is a national laboratory of the U.S. Department of Energy
Office of Energy Efficiency & Renewable Energy
Operated by the Alliance for Sustainable Energy, LLC

This report is available at no cost from the National Renewable Energy Laboratory (NREL) at www.nrel.gov/publications.

Conference Paper
NREL/CP-5000-66011
July 2016

Contract No. DE-AC36-08GO28308

NOTICE

This report is available at no cost from the National Renewable Energy Laboratory (NREL) at www.nrel.gov/publications.

Available electronically at SciTech Connect http:/www.osti.gov/scitech

Available for a processing fee to U.S. Department of Energy and its contractors, in paper, from:

U.S. Department of Energy
Office of Scientific and Technical Information
P.O. Box 62
Oak Ridge, TN 37831-0062
OSTI http://www.osti.gov
Phone: 865.576.8401
Fax: 865.576.5728
Email: reports@osti.gov

Available for sale to the public, in paper, from:

U.S. Department of Commerce
National Technical Information Service
5301 Shawnee Road
Alexandra, VA 22312
NTIS http://www.ntis.gov
Phone: 800.553.6847 or 703.605.6000
Fax: 703.605.6900
Email: orders@ntis.gov

Cover Photos by Dennis Schroeder: (left to right) NREL 26173, NREL 18302, NREL 19758, NREL 29642, NREL 19795.

NREL prints on paper that contains recycled content.

Independent Blade Pitch Controller Design for a Three-Bladed Turbine Using Disturbance Accommodating Control

Na Wang[1], Alan D. Wright[2], and Kathryn E. Johnson[3]
National Renewable Energy Laboratory, Golden, CO 80401 USA

***Abstract*— Two independent pitch controllers (IPCs) based on the disturbance accommodating control (DAC) algorithm are designed for the three-bladed Controls Advanced Research Turbine to regulate rotor speed and to mitigate blade root flapwise bending loads in above-rated wind speed. One of the DAC-based IPCs is designed based on a transformed symmetrical-asymmetrical (TSA) turbine model, with wind disturbances being modeled as a collective horizontal component and an asymmetrical linear shear component. Another DAC-based IPC is designed based on a multiblade coordinate (MBC) transformed turbine model, with a horizontal component and a vertical shear component being modeled as step waveform disturbance. Both of the DAC-based IPCs are found via a regulation equation solved by Kronecker product. Actuator dynamics are considered in the design processes to compensate for actuator phase delay. The simulation study shows the effectiveness of the proposed DAC-based IPCs compared to a proportional-integral (PI) collective pitch controller (CPC). Improvement on rotor speed regulation and once-per-revolution and twice-per-revolution load reductions has been observed in the proposed IPC designs.**

NOMENCLATURE

$v_{1,2,3}$	Wind speeds at blade 1,2,3.
$\beta_{1,2,3}$	Blade 1,2,3 pitch angles.
Ω	Rotor speed.
$x, \bar{x}$	State vector and transformed state vector.
F, Θ	Wind disturbance model matrices.
A, B, B_v, C, D, D_v	Turbine state space model matrices.
T_m, T_β, T_v, T_y	Linear transformation matrices.
T_{mbc}	MBC transformation matrix.
G_x, G_v	DAC controller gains.

I. INTRODUCTION

Significant advanced control techniques for wind turbine fatigue load alleviation have been developed during the past few years for the purpose of reducing the cost of wind energy [1]. The alleviated structural and fatigue loads will significantly decrease the turbine cost by lessening the maintenance requirements and improving overall turbine reliability. Advanced composite materials such as resin-infused woven and stitched fiberglass, which are expected to survive for long periods of time, have been utilized in the blade design to achieve low production cost and also to reduce its operational cost [2], [3]. Modern commercial turbines equipped with individual pitch actuators for each blade for implementation of individual pitch control (IPC) have the potential to reduce the load of rotor blades due to wind speed variations across the rotor plane [4].

Several IPC designs based on linear quadratic Gaussian (LQG) control are presented in [5], [6], which show significant operational load reduction. Preview-based IPC is also proposed in [7], where the feedforward control both with and without the use of multiblade coordinate (MBC) controllers show excellent performance in load mitigation, but only the horizontal wind disturbance model is included in the design. A linear and nonsingular coordinate transformation IPC strategy for two-bladed wind turbines is described in [8], [9], which enables the updating of individual pitch control law and does not rely on rotor azimuth position. Bending moment reductions in tower, shaft torsion, and blade flapwise have been observed in a two-bladed Controls Advanced Research Turbine (CART2) field testing using advanced state-space IPC controllers [10]–[12].

Disturbance accommodating control (DAC) incorporates a predefined waveform model as the internal model and augments it with the turbine state-space model to reduce the wind disturbance effects on the outputs of the wind turbine. The predetermined waveform generator is used to model the unknown persistent disturbances, which will drastically reduce the benefits of active structure control unless the controller can be designed to counteract such disturbances [13], [14]. The studies of DAC for wind turbine load mitigation have been published in the work [15]–[18]. In these works, DACs are found via Moore-Penrose pseudoinverse to minimize the disturbance effect on the system, which can not guarantee zero steady regulation error. A DAC-based extreme wind event controller and a DAC-based speed torque controller have been presented in [19], [20] to regulate rotor speed without steady state error but is only suitable for the waveform model having a single disturbance state.

In this research, the DAC-based IPCs are determined by a regulation equation that is solved via Kronecker product. If solvable conditions are fulfilled, zero regulation steady error can be guaranteed no matter whether the disturbance model is a multistate model or a single-state one. An observer has to be included in the DAC-based IPC loop to estimate the unknown turbine and disturbance states and to construct the internal disturbance model to reject a predetermined wind

[1]Na Wang is with the National Renewable Energy Laboratory, Golden, CO 80401 USA (e-mail: na.wang@nrel.gov).

[2]Alan D. Wright is with the National Renewable Energy Laboratory, Golden, CO 80401 USA (e-mail: alan.wright@nrel.gov).

[3]Kathryn E. Johnson is with the Colorado School of Mines, Department of Electrical Engineering and Computer Science, and Joint Appointee at National Renewable Energy Laboratory, Golden, CO 80401 USA (e-mail: kjohnson@mines.edu).

disturbance. Additionally, the blades of wind turbine experience periodic disturbance due to the combination of gravity force and vertical shear impact on the rotational blades. The once-per-revolution (1P) and twice-per-revolution (2P) are the two dominant periodic frequency disturbances on the blades. In our recent work [9], a DAC-based IPC has been developed on a transformed symmetrical-asymmetrical (TSA) turbine model to mitigate the 1P asymmetrical blade flapwise load and also to regulate the above-rated rotor speed on a two-bladed wind turbine. In this work, we extend the DAC-based IPC on a three-bladed wind turbine, where we apply asymmetrical blade load control at not only the 1P frequency but also at the 2P frequency. Another contribution of this paper is the design of an MBC DAC-based IPC, where an azimuth-averaged MBC transformed turbine model is used for such DAC design. The wind disturbance model contains not only a horizontal collective wind disturbance but also an MBC-transformed vertical shear disturbance, both of which are step waveform.

The remainder of this paper is organized as follows: Section II describes the design of both the TSA-based and the MBC-based DAC IPCs for a three-bladed turbine, together with the description of the turbine model, the wind disturbance model, and the transformed turbine model. Section III shows the experiment environment, including the simulated wind turbine model and the simulated turbulent wind field. Section IV gives the simulation results compared with a proportional-integral (PI) based collective pitch control (CPC). And concluding remarks are given in Section V.

II. DAC-based IPC Design for a Three-bladed Turbine

A. TSA IPC Design

1) Azimuth-Averaged Three-Bladed Turbine Model: The turbine model used for TSA IPC design is a four degrees-of-freedom (DOF) model, which includes three-blade flapwise modes and one rotational rotor mode. We use β_1, β_2, and β_3 as the pitch angles for three blades; v_1, v_2, and v_3 as the prevailing wind speed at the tip of each blade; Ω as the rotor speed; and y_1, y_2, and y_3 as each blade's root flapwize bending moment. A linear continuous-time azimuth-averaged state-space model at a specific operating point can be expressed as

$$\begin{aligned}\Delta\dot{x}(t) &= A\Delta x(t) + B\Delta\beta(t) + B_v\Delta v(t),\\ \Delta y(t) &= C\Delta x(t) + D\Delta\beta(t) + D_v\Delta v(t),\end{aligned} \tag{1}$$

where

$$\beta = \begin{bmatrix}\beta_1,\beta_2,\beta_3\end{bmatrix}^T, v = \begin{bmatrix}v_1,v_2,v_3\end{bmatrix}^T, y = \begin{bmatrix}\Omega, y_1, y_2, y_3\end{bmatrix}^T,$$

$$x = \begin{bmatrix}\text{flapwise bending deflection of blade 1 (m)}\\ \text{flapwise bending deflection of blade 2 (m)}\\ \text{flapwise bending deflection of blade 3 (m)}\\ \text{rotor speed in (rad/s)}\\ \text{flapwise bending velocity of blade 1 (m/s)}\\ \text{flapwise bending velocity of blade 2 (m/s)}\\ \text{flapwise bending velocity of blade 3 (m/s)}\end{bmatrix}.$$

x contains the plant states; β is the control input (i.e., pitch angle vector); y is the plant output; deviations from the operating point are indicated by Δ; and A, B, B_v, C, D, D_v are the continuous-time state-space model matrices with appropriate sizes and are obtained from the FAST linearization process.

2) Wind Disturbance Model: Due to vertical wind shear variations across the rotor plane, the three-bladed wind turbine experiences periodic frequency disturbances. The 1P frequency and 2P frequency are the two most dominant disturbances. The wind disturbance v^{lin} can be modeled as an asymmetrical linear shear component v_d, which is a combined sinusoidal 1P and 2P waveform, and as a horizontal collective wind component v_c, which is a stepwise constant waveform. The wind disturbance model is defined in (2)-(3).

$$\begin{aligned}\Delta\dot{x}_v(t) &= F^{lin}\Delta x_v(t),\\ \Delta v^{lin}(t) &= \Theta^{lin}\Delta x_v(t),\end{aligned} \tag{2}$$

$$\begin{aligned}F^{lin} &= \begin{bmatrix}0 & 1 & 0 & 0 & 0\\ -\Omega_{1P}^2 & 0 & 0 & 0 & 0\\ 0 & 0 & 0 & 1 & 0\\ 0 & 0 & -\Omega_{2P}^2 & 0 & 0\\ 0 & 0 & 0 & 0 & 0\end{bmatrix},\\ \Theta^{lin} &= \begin{bmatrix}k_{1P} & 0 & k_{2P} & 0 & 0\\ 0 & 0 & 0 & 0 & 1\end{bmatrix}, v^{lin} = \begin{bmatrix}v_d\\ v_c\end{bmatrix},\end{aligned} \tag{3}$$

where x_v is the wind disturbance state; Ω_{1P} and Ω_{2P} are the 1P and 2P rotor speeds in rad/s; and k_{1P}, k_{2P} are the weighting coefficients of 1P and 2P contribution, respectively.

3) Transformed Three-Bladed Turbine Model: Since the wind disturbance model (2)-(3) has been defined with output Δv^{lin}, the linear turbine model (1) must therefore be transformed to include Δv^{lin} for DAC design. A set of linear matrix transformations are determined and applied to (1) to get a symmetrical-asymmetrical model to include the wind disturbance model (2)-(3).

For a three-bladed turbine model, the transformation equations are

$$\begin{aligned}x^{lin} &= T_m x, \beta^{lin} = T_\beta \beta,\\ v^{lin} &= T_v v, y^{lin} = T_y y,\end{aligned} \tag{4}$$

where

$$\begin{aligned}T_m &= \begin{bmatrix}\frac{1}{3} & \frac{1}{3} & \frac{1}{3} & 0 & 0 & 0 & 0\\ \frac{2}{3} & -\frac{4}{3} & \frac{2}{3} & 0 & 0 & 0 & 0\\ 0 & 0 & 0 & 1 & 0 & 0 & 0\\ 0 & 0 & 0 & 0 & \frac{1}{3} & \frac{1}{3} & \frac{1}{3}\\ 0 & 0 & 0 & 0 & \frac{2}{3} & -\frac{4}{3} & \frac{2}{3}\end{bmatrix}, T_\beta = \begin{bmatrix}\frac{1}{3} & \frac{1}{3} & \frac{1}{3}\\ \frac{2}{3} & -\frac{4}{3} & \frac{2}{3}\end{bmatrix},\\ T_v &= \begin{bmatrix}\frac{2}{3} & -\frac{4}{3} & \frac{2}{3}\\ \frac{1}{3} & \frac{1}{3} & \frac{1}{3}\end{bmatrix}, T_y = \begin{bmatrix}1 & 0 & 0 & 0\\ 0 & \frac{2}{3} & -\frac{4}{3} & \frac{2}{3}\end{bmatrix};\end{aligned} \tag{5}$$

the transformed control input and the transformed turbine output are

$$\beta^{lin} = \begin{bmatrix}\beta_c, \beta_d\end{bmatrix}^T, y^{lin} = \begin{bmatrix}\Omega, y_{as}\end{bmatrix}^T \tag{6}$$

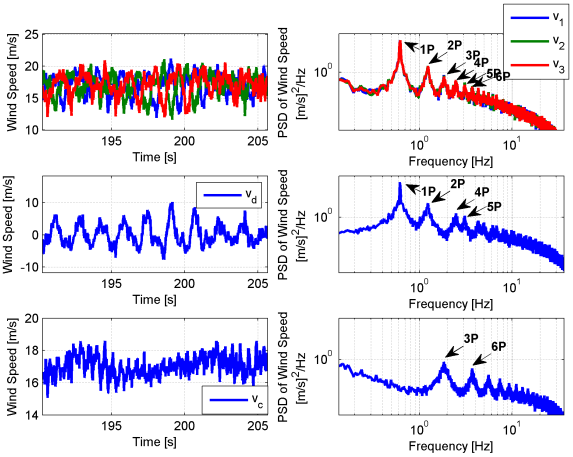

Fig. 1. Transformed collective wind component v_c (shown in the third row) and asymmetrical wind component v_d (shown in the second row) from the transformation matrix T_v in (5) on the three-bladed Controls Advanced Research Turbine's three rotational blade tip wind speeds v_1, v_2 and v_3 (shown in the first row). Both time series (left column) and power spectral densities (PSDs) (right column) are shown.

with β_c being the collective pitch component; β_d being the asymmetrical pitch component; y_{as} being the asymmetrical blade flapwise bending moment; and the transformed states being

$$x^{lin} = \begin{bmatrix} x_1^{lin} \\ x_2^{lin} \\ x_3^{lin} \\ x_4^{lin} \\ x_5^{lin} \end{bmatrix} = \begin{bmatrix} \text{symmetrical flapwise bending deflection (m)} \\ \text{asymmetrical flapwise bending deflection (m)} \\ \text{rotor speed (rad/s)} \\ \text{symmetrical flapwise bending velocity (m/s)} \\ \text{asymmetrical flapwise bending velocity (m/s)} \end{bmatrix}.$$

The vector $(1/3, 1/3, 1/3)$ included in each of the four transformation matrices in (5) is used to obtain the uniform symmetrical components (x_1^{lin}, x_4^{lin}, β_c, and v_c), while the vector $(2/3, -4/3, 1/3)$ is used to get the asymmetrical 1P differential components (x_2^{lin}, x_5^{lin}, β_d, v_d and y_{as}). Then a transformed linear state-space turbine model is given by

$$\begin{aligned} \Delta\dot{x}^{lin}(t) &= A^{lin}\Delta x^{lin}(t) + B^{lin}\Delta\beta^{lin}(t) + B_v^{lin}\Delta v^{lin}(t), \\ \Delta y^{lin}(t) &= C^{lin}\Delta x^{lin}(t) + D^{lin}\Delta\beta^{lin}(t) + D_v^{lin}\Delta v^{lin}(t), \end{aligned} \tag{7}$$

where $A^{lin}, B^{lin}, B_v^{lin}, C^{lin}, D^{lin}, D_v^{lin}$ are obtained from

$$A^{lin} = T_m A T_m^{-1}, B^{lin} = T_m B T_\beta^{-1}, B_v^{lin} = T_m B_v T_v^{-1},$$
$$C^{lin} = T_y C T_m^{-1}, D^{lin} = T_y D T_\beta^{-1}, D_v^{lin} = T_y D_v T_v^{-1}.$$

An example of the effect of the linear transformation matrix T_v on the three-bladed Controls Advanced Research Turbine's (CART's) three rotational blade tip prevailing wind speeds v_1, v_2, v_3 from a turbulent wind field is shown in Fig. 1. The rated rotor speed of CART3 is 37 rpm so the 1P frequency is 0.617 Hz and the 2P frequency is 1.23 Hz. It is seen that the collective wind component v_c contains 3P, 6P, and so on, while the asymmetrical wind component v_d contains 1P, 2P, 4P, 5P, etc., indicating that the 1P and the 2P are the first two dominant asymmetrical disturbance peaks.

Such linear model transformations (4)-(5) enables the application of DAC to reduce both collective wind disturbance and asymmetrical 1P and 2P wind disturbance impact on rotor speed and asymmetrical flapwise bending moment. Note that the turbine's pitch actuator control signals β for use in implementation are obtained by inverse transformation from β^{lin}. However, the proposed linear transformations would result in unbalanced blade loads due to the unequally weighted vector (2/3,-4/3,2/3) included in each of the four transformation matrices (5). Therefore, one blade always has more control impact than the others, which might have unexpected influence on drive-train or yaw system. Another DAC-based IPC is presented in the next section, utilizing an MBC transformation to get a turbine model in the nonrotational frame to avoid such unbalanced transformations.

B. MBC IPC Design

The basic MBC transformation matrix $T(\theta)$ for a three-bladed turbine is defined as

$$T_{mbc}(\theta) = \begin{bmatrix} \frac{1}{3} & \frac{1}{3} & \frac{1}{3} \\ \frac{2}{3}cos(\theta) & \frac{2}{3}cos(\theta+\frac{2\pi}{3}) & \frac{2}{3}cos(\theta+\frac{4\pi}{3}) \\ \frac{2}{3}sin(\theta) & \frac{2}{3}sin(\theta+\frac{2\pi}{3}) & \frac{2}{3}sin(\theta+\frac{4\pi}{3}) \end{bmatrix}, \tag{8}$$

which is an azimuth θ-dependent transformation and is used to transform the three rotational blades into a fixed-coordinate with a uniform component, a vertical tilt component, and a horizontal tilt component [21].

The wind velocity at a height z with a linear vertical shear coefficient α is given by [22].

$$v(z) = v_{ref}\left(1 + \frac{z - z_{ref}}{\phi}\alpha\right), \tag{9}$$

where $v(z)$ is the wind velocity (m/s) at height z (m); z_{ref} and v_{ref} are the referenced height and its wind velocity; and ϕ is the rotor diameter (m). As shown in Fig. 2, a stepwise constant wind file with a '0.4' linear vertical shear coefficient, as defined in (9), marches forward to a spinning wind turbine. The three rotational blade tip wind speeds v_1, v_2, v_3 are 1P sinusoidal waveforms, and the transformed uniform wind component v_u, vertical shear component v_{nc}, and horizontal shear component v_{ns} are step waveforms. Because the disturbance waveforms (v_u, v_{nc}, v_{ns}) do not depend on the azimuth angle θ, all of which are stepwise constant, we can use an azimuth-averaged MBC-transformed state-space model given by (10) to design the DAC IPC.

$$\begin{aligned} \Delta\dot{x}^{mbc}(t) &= A^{mbc}\Delta x^{mbc}(t) + B^{mbc}\Delta\beta^{mbc}(t) \\ &\quad + B_v^{mbc\prime}\Delta v^{mbc\prime}(t), \\ \Delta y^{mbc}(t) &= C^{mbc}\Delta x^{mbc}(t) + D^{mbc}\Delta^{mbc}\beta^{mbc}(t) \\ &\quad + D_v^{mbc\prime}\Delta v^{mbc\prime}(t), \end{aligned} \tag{10}$$

with

$$\beta^{mbc} = \begin{bmatrix} \beta_u \\ \beta_{nc} \\ \beta_{ns} \end{bmatrix}, v^{mbc\prime} = \begin{bmatrix} v_u \\ v_{nc} \\ v_{ns} \end{bmatrix}, y^{mbc} = \begin{bmatrix} y_u \\ y_{nc} \\ y_{ns} \end{bmatrix}, \tag{11}$$

where the three components (i.e., uniform 'u,' vertical tilt 'nc', and horizontal tilt 'ns') for β^{mbc}, $v^{mbc\prime}$, and y^{mbc} are generated. In this research, we design an MBC-based IPC to accommodate v_u and v_{nc}. Therefore, the wind disturbance model (2) can be updated to be

$$F^{mbc} = \begin{bmatrix} 0 & 0 \\ 0 & 0 \end{bmatrix}, \Theta^{mbc} = \begin{bmatrix} 1 & 0 \\ 0 & 1 \end{bmatrix}, v^{mbc} = \begin{bmatrix} v_u \\ v_{nc} \end{bmatrix}, \tag{12}$$

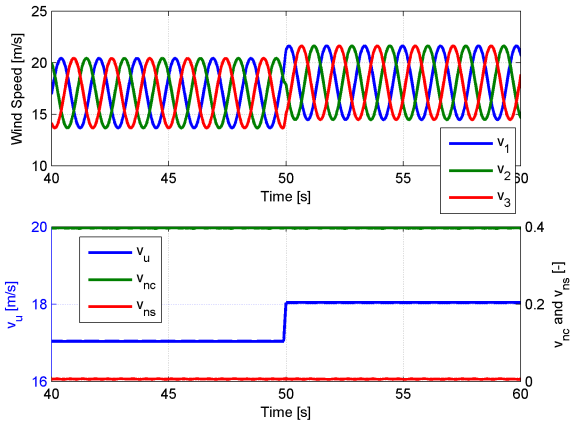

Fig. 2. Transformed uniform wind component v_u stepping from 17 m/s to 18 m/s at 50 s, vertical wind component v_{nc} with a linear shear coefficient of '0.4', and horizontal wind component v_{ns} without shear from the transformation matrix T_{mbc} in (8) on the CART3's three rotational blade tip wind speeds v_1, v_2 and v_3.

where v^{mbc} is a truncated MBC-transformed wind disturbance with only the uniform wind component v_u and the vertical wind component v_{nc}. Then, $B_v^{mbc\prime}$ and $D_v^{mbc\prime}$ are correspondingly truncated to be B_v^{mbc} and D_v^{mbc}.

C. DAC-Based IPC Design

DAC uses a predefined waveform model such as (2) or (12) as part of the feedback control to counteract the wind disturbance effects on the outputs of the wind turbine. In this research, we design two DAC-based IPCs for the turbine models (7) and (10) with two goals: 1) to regulate the rotor speed at the rated value in above-rated wind speed, and 2) to attenuate the blade flapwise loading due to wind vertical shear.

A DAC controller is solvable if the following conditions can be fulfilled [23]:

(a) $v^{\{\cdot\}}$ are persistent disturbances, i.e., the real parts of all eigenvalues in $F^{\{\cdot\}}$ are either positive or zero;
(b) $(A^{\{\cdot\}}, B^{\{\cdot\}})$ is stabilizable;
(c) There exist Π, Γ solution of the following regulation equation

$$\begin{bmatrix} A^{\{\cdot\}} & B^{\{\cdot\}} \\ C^{\{\cdot\}} & D^{\{\cdot\}} \end{bmatrix} \begin{bmatrix} \Pi \\ \Gamma \end{bmatrix} - \begin{bmatrix} \Pi \\ \mathbf{0} \end{bmatrix} F^{\{\cdot\}} = - \begin{bmatrix} B_v^{\{\cdot\}}\Theta^{\{\cdot\}} \\ D_v^{\{\cdot\}}\Theta^{\{\cdot\}} \end{bmatrix}; \quad (13)$$

(d) $\left(\begin{bmatrix} A^{\{\cdot\}} & B_v^{\{\cdot\}}\Theta^{\{\cdot\}} \\ \mathbf{0} & F^{\{\cdot\}} \end{bmatrix}, \begin{bmatrix} C^{\{\cdot\}} & D_v^{\{\cdot\}}\Theta^{\{\cdot\}} \end{bmatrix} \right)$ is detectable,

where $\{\cdot\}$ can be 'lin' or 'mbc' to get a TSA DAC-based IPC design or an MBC DAC-based IPC design. Condition (a) is fulfilled for both cases: the eigenvalues of F^{lin} are $\{\pm j\Omega_{1P}, \pm j\Omega_{2P}, 0\}$ as indicated in (3), and the eigenvalues of F^{mbc} are $\{0, 0\}$ as shown in (12). Other conditions have been checked and are fulfilled. Equation (13) is called the regulation equation, which can be solved via the Kronecker product as

$$\left(I \otimes \begin{bmatrix} A^{\{\cdot\}} & B^{\{\cdot\}} \\ C^{\{\cdot\}} & D^{\{\cdot\}} \end{bmatrix} + F \otimes I \right) vec\left(\begin{bmatrix} \Pi \\ \Gamma \end{bmatrix} \right) = vec\left(- \begin{bmatrix} B_v^{\{\cdot\}}\Theta^{\{\cdot\}} \\ D_v^{\{\cdot\}}\Theta^{\{\cdot\}} \end{bmatrix} \right) \quad (14)$$

with I being the appropriately sized identity matrix. The full state feedback controller given by DAC is

$$\begin{aligned} \Delta\beta^{\{\cdot\}}(t) &= \begin{bmatrix} G_x & G_v \end{bmatrix} \begin{bmatrix} \Delta x^{\{\cdot\}}(t) \\ \Delta x_v^{\{\cdot\}}(t) \end{bmatrix}, \\ G_v &= \Gamma - G_x\Pi, \end{aligned} \quad (15)$$

with G_x, G_v being the controller gains associated with turbine states $x^{\{\cdot\}}$ and disturbance states $x_v^{\{\cdot\}}$, respectively. In order to implement controller (15), $x^{\{\cdot\}}$ and $x_v^{\{\cdot\}}$ should be estimated from an observer. The estimated states $\hat{x}^{\{\cdot\}}$ and $\hat{x}_v^{\{\cdot\}}$ can be given by

$$\begin{aligned} \begin{bmatrix} \Delta\dot{\hat{x}}^{\{\cdot\}}(t) \\ \Delta\dot{\hat{x}}_v^{\{\cdot\}}(t) \end{bmatrix} &= \begin{bmatrix} A^{\{\cdot\}} & B_v^{\{\cdot\}}\Theta^{\{\cdot\}} \\ \mathbf{0} & F^{\{\cdot\}} \end{bmatrix} \begin{bmatrix} \Delta\hat{x}^{\{\cdot\}}(t) \\ \Delta\hat{x}_v^{\{\cdot\}}(t) \end{bmatrix} \\ &\quad + \begin{bmatrix} B^{\{\cdot\}} \\ \mathbf{0} \end{bmatrix} \Delta\beta^{\{\cdot\}}(t) + L\Big(\Delta y^{\{\cdot\}}(t) - \Delta\hat{y}^{\{\cdot\}}(t) \Big), \\ \Delta\hat{y}^{\{\cdot\}}(t) &= \begin{bmatrix} C^{\{\cdot\}} & D_v^{\{\cdot\}}\Theta^{\{\cdot\}} \end{bmatrix} \begin{bmatrix} \Delta\hat{x}^{\{\cdot\}}(t) \\ \Delta\hat{x}_v^{\{\cdot\}}(t) \end{bmatrix} + D^{\{\cdot\}}\Delta\beta^{\{\cdot\}}(t). \end{aligned} \quad (16)$$

with L being the observer gain, which is chosen to ensure that the state error Δe goes to zero quickly in (17). The state error Δe is

$$\Delta e^{\{\cdot\}} = \begin{bmatrix} \Delta x^{\{\cdot\}} - \Delta\hat{x}^{\{\cdot\}} \\ \Delta x_v^{\{\cdot\}} - \Delta\hat{x}_v^{\{\cdot\}} \end{bmatrix},$$

and its dynamics can be shown to satisfy

$$\Delta\dot{e}^{\{\cdot\}}(t) = \left(\begin{bmatrix} A^{\{\cdot\}} & B_v^{\{\cdot\}}\Theta \\ \mathbf{0} & F \end{bmatrix} - L \begin{bmatrix} C^{\{\cdot\}} & D_v^{\{\cdot\}}\Theta \end{bmatrix} \right) \Delta e^{\{\cdot\}}(t). \quad (17)$$

Also, the delayed pitch actuation will degrade the controller's performance. The pitch actuator dynamics can be incorporated into the controller design process to compensate the phase delay introduced by the actuators. More details can be found in [9].

III. Simulation Environment

The CART3, located at the National Wind Technology Center at the National Renewable Energy Laboratory, is used in the simulation study. CART3 is a 600-kW research wind turbine with a rotor diameter of 40 m and hub height of 36.6 m. The rated rotor speed is 37 rpm. FAST [24] is used to model the CART3 with 15 enabled DOFs: the generator mode, the drivetrain mode, the first and second blade flapwise modes for three blades, the first blade edgewise mode for three blades, the first and second tower fore-aft modes, and the first and second tower side-to-side modes.

A 10-min TurbSim-generated [25] wind file with a mean of 18 m/s and a power law exponent of 0.125 is used in the simulations to verify the proposed DAC-based IPC controllers' effectiveness. TurbSim uses the inverse Fourier transformation of a wind spectrum model to numerically simulate the time series of three component wind speed vectors. The wind profiles of the 10-min turbulent wind file at the hub-height are plotted in Fig. 1. The figure shows that in the 10-min turbulent wind case, the periodic frequencies 1P, 2P, 3P, 4P, and so on appear in v_1, v_2, v_3 due to rotor rotation.

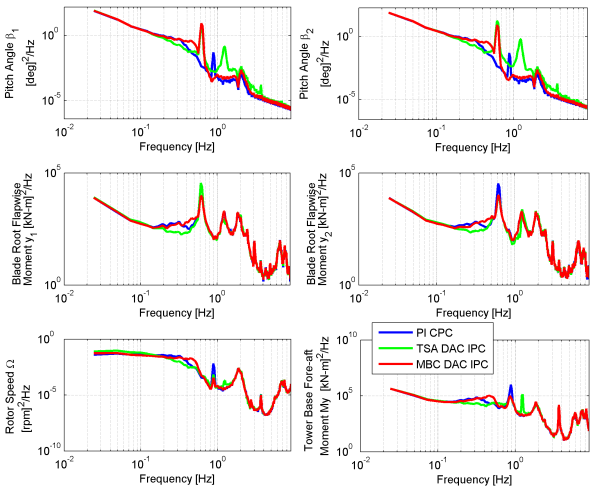

Fig. 3. The PSDs of PI CPC, TSA DAC IPC, and MBC DAC IPC in terms of the pitch angles β_1, β_2, the rotor speed Ω, and the blade flapwise bending moment y_1, y_2 using the TurbSim-generated wind file as shown in Fig. 1. The tower base fore-aft bending moment M_y is shown as well. β_3 and y_3 are not shown, because they are similar to β_1 and y_1.

IV. Simulation Results and Discussion

The two DAC independent pitch controllers presented in Section II are compared to a PI-based collective blade pitch controller (PI CPC), which utilizes a feedback rotor speed error signal to simultaneously update blade pitch control commands [26].

The power spectral densities (PSDs) of selected signals from simulation results in the TurbSim-generated wind file (plotted in Fig. 1) are shown in Fig. 3.

Compared to the PI collective pitch controller, the independent pitch controllers (TSA DAC IPC and MBC DAC IPC) had 1P (0.61 Hz) pitch control authorities in the three blades $(\beta_1, \beta_2, \beta_3)$ to mitigate the 1P loading in the three-blade root flapwise bending moments (y_1, y_2, y_3). The TSA-based independent pitch controller had an additional 2P control authority because of the predetermined wind disturbance model including a 2P mode as indicated in (2)-(3). Fig. 3 shows significant 1P load reduction existed in both the DAC-based independent pitch controllers. Also, the TSA DAC IPC had the additional 2P load reductions as designed. However, the TSA DAC IPC also had imbalanced 1P load reductions on signals y_1, y_2, y_3 (i.e., y_2 has the lowest 1P frequency peak). This imbalance results from the linear transformations (4)-(5) that construct the asymmetrical components u_d, β_d, y_d using the unequal weighing vector. The 'four third' weighting coefficient can be placed to other blades, then the corresponding 1P peak load for that blade will be attenuated. Such imbalanced blade load reductions resulted in a worse load on the yaw moment y_{yaw} as shown in Fig. 4, where two peaks at 1P and 2P, respectively, appeared in the PSD of TSA DAC IPC's yaw moment signal. Also, there was a peak frequency at 0.89 Hz, which was the first tower mode. In the DAC-based independent controllers, a tower mode notch filter has been placed in the collective

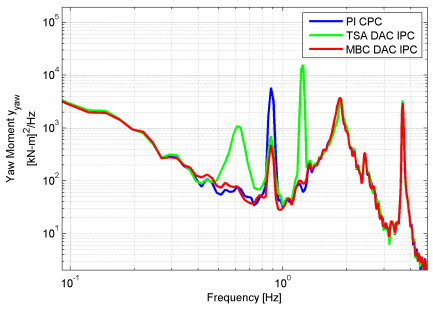

Fig. 4. The PSDs of PI CPC, TSA DAC IPC, and MBC DAC IPC in terms of the yaw moment y_{yaw}.

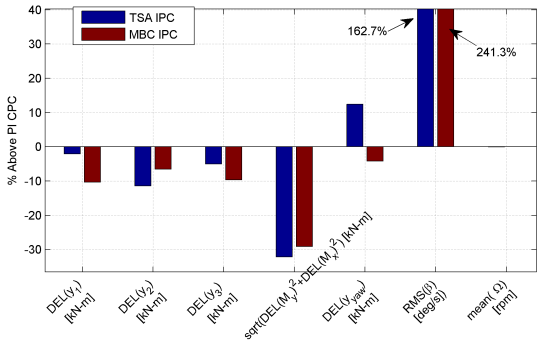

Fig. 5. Statistics of the DAC IPCs percentage over the PI CPC.

control loop (β_c or β_u) to reduce the risk of the tower mode coupling with the 1P frequency. Because the tower side-to-side mode coupled with the rotor rotation mode, insufficient damped tower mode would be transfered into blade flapwise bending moment via rotor rotation.

The statistical results, including the fatigue damage equivalent loads (DELs) for the three-blade root flapwise bending moments, the tower base fore-aft and side-to-side bending moments, the yaw moment, the root mean square (RMS) value of pitch rate, and the mean rotor speed value, are shown in Fig. 5. The tower DELs have been reduced around 30% in both independent pitch controllers, partially for the sake of the tower mode notch filters placed in the control loops and partially due to the reduced magnitude in the tower fore-aft bending moment over lower frequencies as indicated in Fig. 3. The maximum blade DELs have been attenuated by 2.03% and 6.57% for the TSA- and MBC-based DAC IPCs, respectively. The MBC-based DAC IPC resulted in smaller blade DELs due to the magnitude being reduced almost equally for the three blades. Because of the imbalanced blade load reduction in the TSA-based DAC IPC, the yaw moment DEL was increased by 12.4%, while it was reduced by 4.14% in the MBC-based IPC. The pitch rate increased substantially because more pitch actuation was required in the independent pitch controllers. The rotor speed regulations in the independent pitch controllers were comparable to the PI collective pitch controller.

V. Conclusion and Future work

In this paper, two multi-input and multi-output DAC-based independent pitch controllers were developed to reduce the wind disturbance effects on the rotor speed and the asymmetrical flapwise loading when the wind speed was above rated. The DAC controllers were designed based on a TSA-transformed turbine model and an MBC-transformed turbine model, respectively. The predetermined wind models with sinusoidal waveform and step waveform were incorporated in the state-space controller. Actuator dynamic was included in the design process to compensate the phase delay introduced by the actuator model. Simulation experiments were conducted in a 10-min turbulent wind field and CART3 FAST turbine model. The PI collective pitch controller was selected as a baseline to verify the effectiveness of the proposed independent control strategies.

Both the TSA DAC and the MBC DAC independent pitch controllers outperform the PI collective pitch controller on 1P blade flapwise load reduction. The DAC-based IPCs have a comparable rotor speed regulation as the PI CPC. The symmetric-asymmetric linear model transformations in the TSA-based DAC IPC are effective to decouple control loops for utilizing DAC approach but result in imbalanced blade flapwise load reductions, while the azimuth-averaged MBC transformation reduces such imbalance in blade loading. The embedded sinusoidal waveform and step waveform are the internal models that associates with the DAC feedback controller to achieve the wind disturbance accommodation on the turbine outputs.

Overall, the proposed DAC-based independent pitch controllers have the potential to reduce the wind disturbance effects on rotor speed and asymmetrical flapwise loading due to vertical wind shear in above-rated wind speed. Future work will focus on a higher periodic disturbance model coupled into the MBC DAC-based IPC to address asymmetrical blade flapwise load reduction in a wider frequency range. Also, we would like to design a DAC-based IPC based on an azimuth-dependent periodic MBC turbine model to further enhance balanced blade loading.

Acknowledgments

This work was supported by the U.S. Department of Energy under Contract No. DE-AC36-08GO28308 with the National Renewable Energy Laboratory. Funding for the work was provided by the DOE Office of Energy Efficiency and Renewable Energy, Wind and Water Power Technologies Office.

References

[1] L. Pao and K. Johnson, "A Tutorial on the Dynamics and Control of Wind Turbines and Wind Farms," in *Proceedings of the American Controls Conference*, (St. Louis, MO), June 2009.

[2] T. D. Ashwill, "Materials and Innovations for Large Blade Structures: Research Opportunities in Wind Energy Technology," in *Proceedings of 50th AIAA Structures, Structural Dynamics, and Materials Conference*, (Palm Springs), May 2009.

[3] G. Abumeri and F. Badi, *Advanced Composite Wind Turbine Blade Design Based on Durability and Damage Tolerance*. Long Beach, CA, USA: Alpha STAR Corporation, Feb. 2012.

[4] K. Selvam, S. Kanev, J. Wingerden, T. Engelen, and M. Verhaegen, "Feedback-feedforward Individual Pitch Control for Wind Turbine Load Reduction," *International Journal of Robust and Nonlinear Control*, vol. 19, pp. 72–91, Apr. 2008.

[5] E. A. Bossanyi and G. Hassan, "Individual Blade Pitch Control for Load Reduction," *Wind Energy*, vol. 6, pp. 119–128, 2003.

[6] K. Selvam, *Individual Pitch Control for Large Scale Wind Turbines*. Netherlands: Energy Research Center of the Netherlands, 2007.

[7] J. Laks, L. Pao, A. D. Wright, N. Kelley, and B. Jonkman, "Blade Pitch Control with Preview Wind Measurements," in *Proceedings of American Institute of Aeronautics and Astronautics*, (Orlando, FL), Jan. 2010.

[8] E. van Solingen and J. W. van Wingerden, "Linear Individual Pitch Control Design for Two-bladed Wind Turbines," *Wind Energy*, vol. 18, pp. 677–697, April 2015.

[9] N. Wang, A. D. Wright, and M. Balas, "Disturbance Accommodating Control based Independent Blade Pitch Control Design on CART2," in *34th Wind Energy Symposium, AIAA Science and Technology Forum and Exposition 2016*, (San Diego, CA), Jan. 2016.

[10] K. A. Stol, W. Zhao, and A. D. Wright, "Individual Blade Pitch Control for the Controls Advanced Research Turbine CART," *Journal of Solar Energy Engineering*, vol. 128, pp. 498–505, 2006.

[11] A. D. Wright, L. J. Fingersh, and K. A. Stol, "Testing Controls to Mitigate Fatigue Loads in the Controls Advanced Research Turbine," in *17th Mediterranean Conference on Control and Automation*, (Thessaloniki, Greece), June 2009.

[12] A. Wright, P. Fleming, and J. van Wingerden, "Refinements and Tests of an Advanced Controller to Mitigat Fatigue Loads in the Controls Advanced Research Turbine," in *49th AIAA Aerospace Sciences Meeting*, (Orlando, FL), 2011.

[13] Y. J. Lee, M. J. Balas, and H. Waites, "Disturbance Accommodating Control for Completely Unknown Persistent Disturbances," in *Proceedings of the American Controls Conference*, (Seattle, WA), June 1995.

[14] M. J. Balas, "Active Control of Persistent Disturbances in Large Precision Aerospace Structures," in *Proceedings of SPIE 1303, Advances in Optical Structure Systems*, (Seattle, WA), Oct. 1990.

[15] A. D. Wright, *Modern Control Design for Flexible Wind Turbines*. Golden, CO, USA: National Renewable Energy Laboratory, 2004.

[16] K. Stol and M. Balas, "Periodic Disturbance Accommodating Control for Blade Load Mitigation in Wind Turbines," *Journal of Solar Energy Engineering*, vol. 125, pp. 379–385, Nov. 2003.

[17] M. Hand, K. E. Johnson, L. J. Fingersh, and A. D. Wright, *Advanced Control Design and Field Testing for Wind Turbines at the National Renewable Energy Laboratory*. Golden, CO, USA: National Renewable Energy Laboratory, May 2004.

[18] H. Namik and K. Stol, "Individual Blade Pitch Control of a Spar-buoy Floating Wind Turbine," *IEEE Transactions on Control System Technology*, vol. 22, no. 1, pp. 214–223, Jan. 2013.

[19] A. Pace and K. E. Johnson, "LIDAR-based Extreme Event Control to Prevent Wind Turbine Overspeed," in *Proceedings of the AIAA Aerospace Sciences Meeting and Exhibit*, (Grapevine, TX), Jan. 2013.

[20] N. Wang, A. D. Wright, K. E. Johnson, and C. E. Carcangiu, "Lidar-assisted Wind Turbine Feedforward Torque Controller Design Below Rated," in *Proceedings of American Control Conference*, (Portland, OR), pp. 3728–3733, June 2014.

[21] G. Bir, "Multi Blade Coordinate Transformation and its Application to Wind Turbine Analysis," in *ASME Wind Energy Symposium*, (Reno, Nevada), June 2008.

[22] P. J. Moriarty and A. C. Hansen, *AeroDyn Theory Manual*. Golden, CO, USA: National Renewable Energy Laboratory, Jan. 2005.

[23] B. Francis, "The Linear Multivariable Regulator Problem," *SIAM Journal on Control and Optimization*, vol. 15, no. 3, pp. 121–127, May 1977.

[24] J. Jonkman and M. L. Buhl, *FAST User's Guide*. Golden, CO, USA: National Renewable Energy Laboratory, 2005.

[25] N. D. Kelley and B. J. Jonkman, *Overview of the Turbsim Stochastic Inflow Turbulence Simulator: Version 1.21 (Revised Feb. 1, 2007)*. Golden, CO, USA: National Renewable Energy Laboratory, April 2007.

[26] K. E. Johnson, L. J. Fingersh, and A. D. Wright, *Controls Advanced Research Turbine: Lesssons Learned during Advanced Controls Testing*. Golden, CO, USA: National Renewable Energy Laboratory, 2005.